JOURNAL OF CATALYSIS 91, 142–154 (1985)

Studies of the Surface Coverage of Unsupported Ruthenium by Carbon- and Hydrogen-Containing Adspecies during CO Hydrogenation

PHILIP WINSLOW AND ALEXIS T. BELL

Materials and Molecular Research Division, Lawrence Berkeley Laboratory, and Department of Chemical Engineering, University of California, Berkeley, California 94720

Received May 21, 1984; revised August 20, 1984

Isotopic tracer techniques have been used to identify the coverages of adsorbed CO, carbon, and hydrogen on the surface of unsupported Ru powder during CO hydrogenation. The coverage by adsorbed CO was close to a monolayer. Two forms of carbon were identified, C_α and C_β, which differed in their dynamics of formation, and conversion to hydrocarbons. C_α is more reactive than C_β and is the principal intermediate in the synthesis of methane and C_2^+ hydrocarbons. C_β accumulates continuously during the reaction but does not strongly inhibit the adsorption of CO or hydrogen. A remarkable finding is that under reaction conditions, nearly a monolayer of hydrogen is adsorbed on the Ru surface. Additional hydrogen is found to be associated with the β-form of carbon, such that the D/C ratio of C_β is between 1.8 and 2.4.

INTRODUCTION

Recent investigations of hydrocarbon synthesis from CO and H_2 over Ru and other Group VIII metals have identified carbon as an important surface intermediate (*1–4*). The amount, structure, and reactivity of the deposited carbon have been shown to vary significantly with reaction conditions. It is found, in general, that the rate of carbon deposition accelerates with increasing temperature and decreasing H_2/CO ratio of the synthesis gas. High temperatures also promote the conversion of reactive carbidic carbon to unreactive graphitic carbon.

Considerable information concerning the kinetics of carbon formation and consumption, and the existence of different modifications of carbon on Ru catalysts has been gained through the use of isotopic tracers (i.e., ^{13}CO and $C^{18}O$). Work by Biloen *et al.* (*5, 6*) and Cant and Bell (*7*) has shown that the dissociation of adsorbed CO appears to be irreversible under conditions of CO hydrogenation. In addition, the carbon formed is highly reactive and can produce methane as well as higher molecular weight hydrocarbons. Tamaru and co-workers (*8, 9*) have suggested that a part of the carbon inventory on the catalyst is in the form of hydrocarbon chains attached to the metal surface. It was proposed that these species can resupply the catalyst surface with single carbon atom species by scission of the carbon–carbon bonds in the chains.

More recently, Winslow and Bell (*10*) have shown that there can be two distinctly different forms of carbon present on the surface of Ru/SiO_2 catalyst. The two forms, designated C_α and C_β, exhibit quite different kinetics of formation and consumption. The surface coverage of C_α rapidly comes to a steady-state value. The steady-state rate of methane formation is found to be a linear function of the C_α coverage. The inventory of C_β is considerably larger than that of C_α and grows continually with time under reaction conditions. The beta-form of carbon is less reactive than C_α. Characterization of C_α and C_β by solid-state NMR has been reported by Duncan *et al.* (*11*). Their

0021-9517/85 $3.00

results suggest that C_α consists of isolated carbon atoms bonded to Ru atoms either on or below the surface of the metal crystallites. The NMR peak for C_β was originally ascribed to carbon bonded to silica atom of the support; however, more recent work (*12*) indicates that the C_β peak is better assigned to a combination of alkyl groups and highly mobile nonhydrogenated species. These studies also revealed the presence of a small amount of graphite-like carbon.

In contrast to what is known about the concentrations of adsorbed CO and carbon on the surface of Ru catalysts, little is yet known about the concentrations of adsorbed H_2. McKee (*13*) has observed that when H_2 and CO are coadsorbed on Ru powder at temperatures from 318 to 427 K, more than two monolayer equivalents of H-atoms are taken up, together with nearly a monolayer of CO. Since the amount of H_2 adsorbed in the presence of CO was nearly twice that adsorbed in the absence of CO, McKee suggested that adsorbed CO strengthens the adsorption of H_2.

This paper presents the results of an isotopic tracer study of CO hydrogenation over Ru powder. The aim of this work was to identify the catalyst coverage by hydrogen, as well as by CO and carbon, during CO hydrogenation. Unsupported Ru was used to facilitate the determination of adsorbed H_2 by eliminating the complications caused by hydroxyl groups present at the surface of an oxide support.

EXPERIMENTAL

Experiments were carried out with a small glass reactor, containing 500 mg of catalyst, heated in a fluidized sand bath. Gas for the reactor was supplied from a manifold made up of two equivalent branches. The two branches are connected to a low dead-volume valve which is used to select the feed stream delivered to the reactor. The reaction products were analyzed on line with a mass spectrometer connected to a microcomputer-based data acquisition system. Samples of the product were analyzed occasionally by gas chromatography to determine the concentrations of higher molecular weight products. Further details concerning the experimental apparatus are given in refs. (*7, 10*).

The catalyst was a ruthenium powder (99.9%) purchased from MacKay A.D., Inc. The dispersion of this material was measured by H_2 chemisorption, CO titration, and CO displacement (*10*), following reduction in flowing H_2 at 673 K. Each technique gave a dispersion of 0.35 ± 0.05%. H_2, D_2, and ^{12}CO were purified using the techniques described in refs. (*7, 10*). ^{13}CO (83% $^{13}C^{16}O$, 17% $^{13}C^{18}O$) and $C^{18}O$ (99% $^{12}C^{18}O$, 1% $^{12}C^{16}O$) were obtained from Liquid Carbonic, and were used without further purification.

All experiments described in this paper were performed using simple variations of the following gas delivery sequence: (i) reduction of the catalyst with H_2 or D_2 to produce a clean catalyst surface; (ii) reaction of D_2 (or H_2) and ^{13}CO (or ^{12}CO) for 30 to 300 s, to accumulate surface carbons with the desired isotopic label (e.g., ^{13}C or ^{12}C); (iii) substitution of adsorbed ^{13}CO (or ^{12}CO) by ^{12}CO, to allow for differentiation between the surface concentrations of adsorbed carbon and CO; (iv) purging with Ar to quench the reaction; and (v) reduction of all adsorbed species with D_2 (or H_2), to quantitatively remove adsorbed carbon as $^{13}CD_4$ (or $^{13}CH_4$), adsorbed ^{12}CO as $^{12}CD_4$ (or $^{12}CH_4$), and adsorbed deuterium (or hydrogen) as HD. More detailed descriptions of the gas delivery sequence are given in the Results section and in the captions to the figures.

RESULTS

Surface Concentrations of Carbon- and Hydrogen-Containing Species

Each experiment was initiated by reducing the catalyst in D_2 for 2 hr before switching in the mixture of D_2 and ^{13}CO. As seen in Fig. 1, the turnover frequency of $^{13}CD_4$ formation is very high initially, but declines

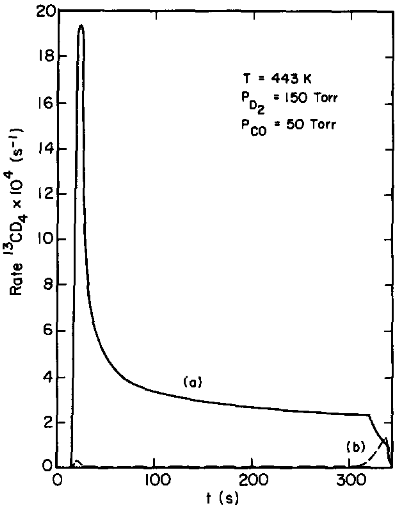

FIG. 1. The rate of $^{13}CD_4$ formation during the following sequences: (a) $D_2 \rightarrow D_2$, ^{13}CO (300 s) $\rightarrow D_2$, ^{12}CO (30 s) $\rightarrow$ Ar (15 s), (b) $D_2 \rightarrow D_2$, ^{12}CO (300 s) $\rightarrow D_2$, ^{13}CO (30 s) $\rightarrow$ Ar (15 s).

to 3×10^{-4} s^{-1} after the first 100 s of reaction. The first 15 s of the transient in the rate of $^{13}CD_4$ formation is accompanied by a transient increase in the partial pressure of D_2, due to the displacement of adsorbed D_2 by the adsorption of CO as seen in Fig. 2. The amount of D_2 displaced is 1.5 monolayer equivalents. The total amount of D_2 adsorbed prior to CO adsorption is about 2.3 monolayer equivalents. The large excess in adsorbed D_2 is presumably due to physical adsorption. However, about 0.8 of a monolayer remains after exposure to CO. This suggests that during the first 15 to 30 s after the introduction of synthesis gas, the surface of the catalyst undergoes a rapid readjustment. The subsequent slow decrease in the rate of $^{13}CD_4$ formation is very likely due to the accumulation of carbon, as discussed later.

Gas chromatographic analysis of the products indicated the presence of C_2 through C_7 hydrocarbons in addition to methane. These products followed a Schulz–Flory distribution characterized by a probability of chain growth, α, of 0.65. The predominant nonhydrocarbon product observed was D_2O. Some CO_2 was also observed, but its concentration never exceeded 5% of the CO converted to hydrocarbons.

When the feed is switched from a mixture of D_2 and ^{13}CO to a mixture of D_2 and ^{12}CO, of equivalent composition, the rate of $^{13}CD_4$ formation begins to decline exponentially, as may be seen in Fig. 1. Independent experiments using infrared spectroscopy with silica-supported ruthenium catalysts have shown that within the first 4 s of the introduction of ^{12}CO, virtually all of the adsorbed ^{13}CO is exchanged for ^{12}CO (*7, 10*). This means that the $^{13}CD_4$ formed during the period that the catalyst is exposed to the D_2–^{12}CO mixture arises from the reaction of adsorbed ^{13}C-carbon rather than the reaction of adsorbed ^{13}CO. The form of adsorbed ^{13}C undergoing reaction during this period is designated C_α. Figure 3 indicates that the kinetics of $^{13}CD_4$ formation from C_α are first order in the surface coverage by C_α. By fitting a first-order rate expression to the data shown in this figure, it was estimated that the coverage by C_α immediately prior to the introduction of the D_2–^{12}CO mixture was 0.009 of a Ru monolayer. This estimate represents a lower bound since, as discussed below, 90% of the C_α is con-

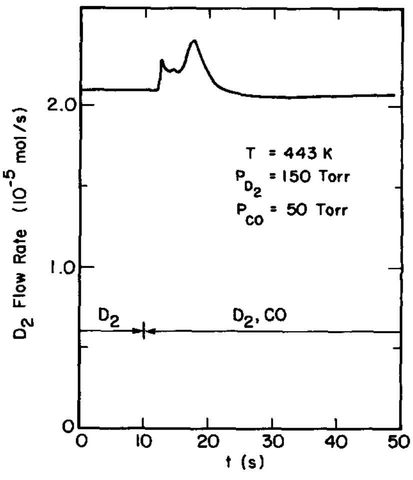

FIG. 2. Transient of D_2 displaced from catalyst surface by exposure to ^{13}CO.

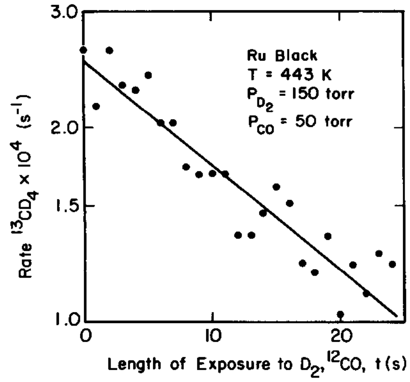

FIG. 3. First order decline in $^{13}CD_4$ rate during D_2, ^{12}CO exposure after the following sequence: $D_2 \rightarrow D_2$, ^{13}CO (300 s) $\rightarrow D_2$, $^{12}CO(t)$.

verted to C_2^+ hydrocarbons. Correcting for the conversion of C_α to higher molecular weight products raises the estimate of the C_α coverage to about 0.07.

Following the period of time under steady-state reaction conditions and the exchange of adsorbed ^{13}CO for ^{12}CO, the catalyst was flushed with argon for 15 s, and then reduced in a flow of D_2. The resulting transient in $^{13}CD_4$ is designated $^{13}CD_4/C_s$ and is shown in Fig. 4. Only small amounts of higher hydrocarbons were observed during reduction. Thus, the integral under the $^{13}CD_4/C_s$ transient represents the total amount of ^{13}C-labeled adsorbed carbon on the catalyst. None of the adsorbed ^{13}CO present at the outset of the experiment contributes to the transient, since all of the adsorbed ^{13}CO was displaced during the exposure to the D_2–^{12}CO mixture. Part of the small shoulder occurring within the first 10 s of the transient in Fig. 4 can be attributed to the reduction of C_α remaining on the catalyst following the exposure to D_2–^{12}CO. This interpretation is based on observations made during similar studies using Ru/SiO_2 catalysts (*7, 10*). The less reactive adsorbed carbon removed following 10 s of reduction has been designated as C_β.

The amount of CO adsorbed on the catalyst under reaction conditions was determined in a manner virtually identical to that used to determine the amount of adsorbed carbon. The only difference in the procedure was that the reaction was first run in D_2 and ^{12}CO, and the adsorbed ^{12}CO was then displaced with ^{13}CO by exposing the catalyst for 30 s to a mixture of D_2 and ^{13}CO. During the exposure to the D_2–^{13}CO mixture, the rate of $^{13}CD_4$ increased in a manner exactly opposite to the decrease observed when the order of introduction of ^{13}CO and ^{12}CO is reversed (see Fig. 1). The curve labeled $^{13}CD_4/CO_s$ in Fig. 4 represents the transient in $^{13}CD_4$ produced by the reduction of ^{13}CO to $^{13}CD_4$ with D_2 during the last step of the sequence. The rate of reduction is slow initially and does not reach a maximum value until about 22 s after the flow of D_2 is initiated. It is also noted that the shape of the $^{13}CD_4/CO_s$ transient is distinctly different from that of the $^{13}CD_4/C_s$ transient. The small shoulder occurring within the first 10 s of the transient observed during the reduction adsorbed CO, seen in Fig. 4, includes a contribution from the conversion of a small amount of adsorbed ^{13}CO to C_α during the exposure to D_2–^{13}CO. The remaining part of the transient is due to reduction of the adsorbed CO.

The $^{13}CD_4/C_s$ and $^{13}CD_4/CO_s$ transients peak at times long after the introduction of

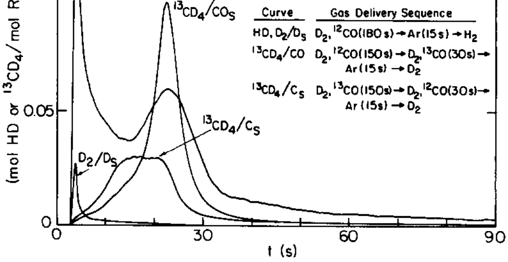

FIG. 4. Transient responses observed during the titration of catalyst surface with D_2 (or H_2) following a period under reaction conditions. Here and in Figs. 5a, 5b, 5c, 8, 10, and 12, *t* is the length of time the adsorbed species react with D_2 (or H_2).

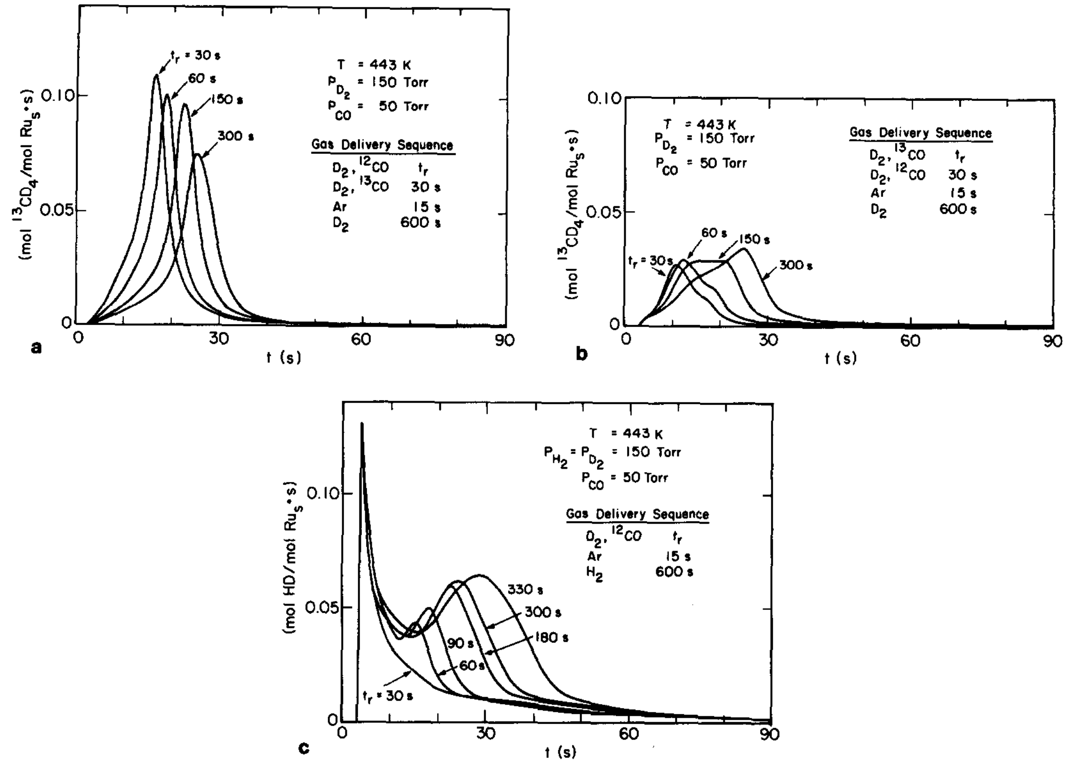

FIG. 5. Effect of varying lengths of time under reaction conditions on CO_s, C_s, and D_s transients: (a) CO_s, (b) C_s, (c) D_s.

D_2 (or H_2). Since the response time of the mass spectrometer system for a step-function change in gas composition is <1 s, the slow rise of the two transients reflects the intrinsic dynamics of the surface reactions. For example, the delayed maximum in the rates of $^{13}CD_4$ formation from adsorbed ^{13}CO can be attributed to the increase in the availability of vacant sites for dissociation as more and more of the surface is cleared of adsorbed species. Initially, θ_v is small but θ_{CO} is high, but late in the reaction θ_v is high and θ_{CO} is small. Consequently, the product $\theta_{CO}\theta_v$ passes through a maximum.

The amount of deuterium on the catalyst surface was measured by exposing the catalyst to a mixture of D_2 and ^{12}CO, flushing the reactor with Ar for 15 s and then reducing off all of the species remaining on the catalyst with H_2. No mixed H/D isotopes of methane were observed during the reduction period and the only products observed to contain deuterium were HD and D_2. The responses for these products are illustrated in Fig. 4. The HD transient is composed of two parts: a very sharp peak with an extended tail and a broad peak centered at about 23 s. The D_2 transient is much smaller than the HD transient. The shapes of the first peak of the HD transient, and of the D_2 transient, are very similar to those observed when H_2 is used to displace adsorbed D-atoms from the surface of Ru powder, in the absence of any adsorbed CO or carbon. This suggests that the initial peak of the HD transient, and all of the D_2 transient shown in Fig. 4, are due to the displacement of D-atoms from the catalyst metal surface.

The effects of time under reaction conditions on the $^{13}CD_4/CO_s$, $^{13}CD_4/C_s$, and HD/D_s transients are presented in Figs. 5a, b,

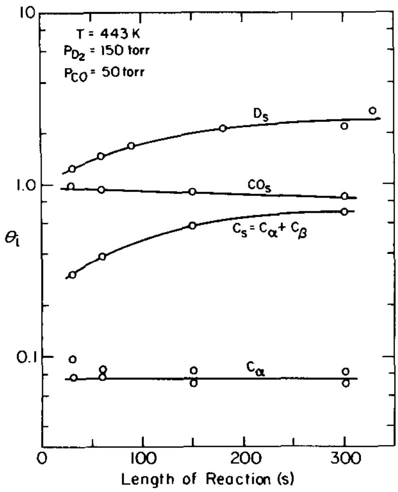

FIG. 6. Effect of reaction time on the coverages by C_α, C_s, CO_s, and D_s. The quantities of θ_{CO_s}, θ_{C_s}, and θ_{O_s} are obtained by integrating the transients in Figs. 5a–c. The quantity θ_{C_α} is obtained from an analysis of transients similar to that shown in Fig. 2.

and c, respectively. The surface concentrations of adsorbed CO, C, and D, determined by the integration of these transients are shown in Fig. 6. In this figure, the concentration of each species is scaled to the concentration of exposed Ru atoms and represented in terms of monolayer equivalents.

The $^{13}CD_4/CO_s$ transient, seen in Fig. 5a, shifts to longer reduction times as the time under reaction conditions increases, indicating a decrease in the activity of the catalyst for reducing CO to methane. For short reaction times, Fig. 6 shows that θ_{CO} is approximately 1.0, but as the duration of reaction increases, θ_{CO} decreases slowly, reaching a value of about 0.85 after 300 s. This suggests that about 15% of the initially adsorbed CO is displaced by other species as the reaction progresses.

Figure 5b shows that the center of the $^{13}CD_4/C_s$ transient shifts to longer times, and the distribution of heights of the three peaks making up the transient changes, the longer the catalyst is held under reaction conditions. These changes are accompanied by an increase in the total carbon inventory. As seen in Fig. 6, the value of θ_{C_s} increases from 0.27 after 30 s of reaction to 0.69 after 300 s of reaction.

The amount of carbon corresponding to C_α determined from the analysis of the transients in $^{13}CD_4$ during exchange between ^{13}CO and ^{12}CO, is also indicated in Fig. 6. It is seen that the inventory of this species is always a modest fraction of the total carbon inventory, and remains constant with time under reaction conditions.

The time under reaction conditions also influences the HD/D_s transient. As seen in Fig. 5c, the transient following 30 s of reaction consists of a single sharp peak, the shape of which is similar to that observed when the displacement of adsorbed deuterium is carried out in the absence of adsorbed CO. This peak is therefore attributed to deuterium adsorbed on the metal surface, and is termed D_α. As the time under reaction conditions increases, the D_α peak remains unchanged and a second peak, designated D_β, appears. The position of this peak shifts to longer times and the peak intensity increases with reaction time.

Figure 6 shows that the total inventory of deuterium on the catalyst is large in all cases and grows monotonically as the time under reaction conditions increases. By extrapolating to the initial time of reaction, an estimate can be attained for the coverage by D_α. A value of ~0.9 is obtained by this means, which is in good agreement with the value of 0.8 estimated earlier from the data presented in Fig. 2. Since the coverage by D_α is independent of the time under reaction conditions, the inventory of D_β can be determined by subtracting the coverage by D_α from the total inventory of deuterium. The correspondence in the rate of growth of the inventory of D_β with that for total carbon strongly suggests that the β-form of deuterium is associated with the β-form of carbon. Working on this assumption, one can readily calculate D_β/C_β. This stoichiometric ratio is plotted in Fig. 7 and is seen to vary between 1.8 and 2.4.

The possibility that C_β and D_β are due to

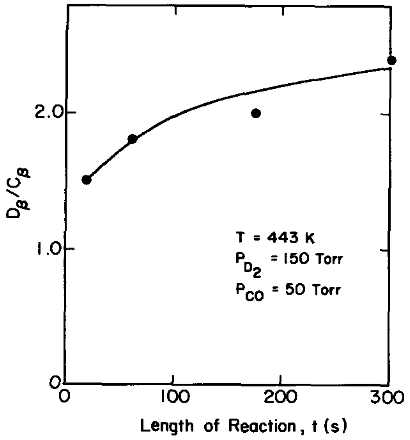

FIG. 7. Variation in D_β/C_β ratio with increasing length of time under reaction conditions.

the accumulation of high-molecular-weight hydrocarbons can be ruled out, since the rate of formation of these products is insufficient to account for the amount of carbon accumulated. If one assumes that all of the hydrocarbons above C_6 remain on the catalyst, the carbon accumulation after 300 s of reaction would correspond to 0.26 monolayer equivalents. Figure 6, however, shows that the actual accumulation of carbon species after 300 s of reaction is 0.69 monolayer equivalents.

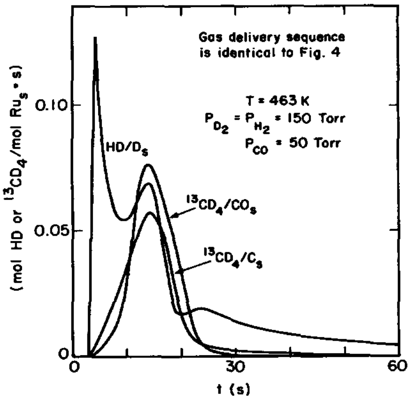

FIG. 8. Transient response observed during titration of catalyst surface with D_2 (or H_2) following a period under reaction conditions at 463 K.

TABLE 1

T (K)	θ_D[a]	θ_C[b]	θ_{CO}	D_β/C_β
443	2.4	0.7	0.8	2.4
463	1.7	0.7	0.8	1.3

[a] Total of all forms of deuterium.

[b] Total of all forms of carbon.

An increase in the temperature from 443 to 463 K has a drastic effect on the reduction transients as can be seen by comparing Figs. 4 and 8. Higher temperatures cause a compression of all transients to shorter reduction times. The quantities of the different surface species are summarized in Table 1. An increase in temperature has no effect on the concentrations of adsorbed CO and C but results in a substantial decrease in the concentration of adsorbed deuterium, predominantly from the D_β pool. As a consequence, the D/C ratio of C_β is 50% lower at 463 than at 443 K.

Isotope Effects

From measurements of the rates of CO hydrogenation with H_2 and D_2, the steady-state isotope effect on methane production after 300 s of reaction was determined to be: $N_{CD_4}/N_{CH_4} = 1.8$. This is in good agreement with the value of 2.2 measured by McKee (*13*) for methane synthesis over a Ru powder, and is at the upper end of the range of values, 1.0 to 1.8, reported by other authors (*14–16*) for methane synthesis over supported Ru.

The H_2–D_2 isotope effect on the synthesis rates of C_1 through C_6 products is shown in Fig. 9. The distributions resulting from D_2–CO and H_2–CO parallel each other, and the probability for chain growth is 0.65 in both cases. This result is to be contrasted with the observations of Kellner and Bell (*14*) who observed a decrease in the isotope effect from 1.5 to 1.0 with increasing carbon number, for synthesis over a Ru/Al_2O_3 catalyst.

An isotope effect is also observable during reduction of species on the catalyst surface. In the experiment shown in Fig. 4,

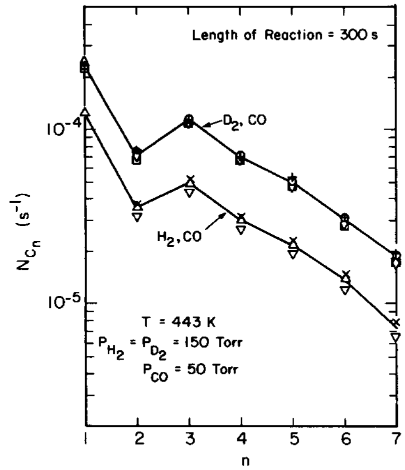

FIG. 9. Influence of $H_2:D_2$ isotope effect on the Schultz–Flory hydrocarbon distribution.

each reduction transient was preceded by a period of reaction in D_2 and CO. For C and CO, the surface was reduced with D_2 to generate a $^{13}CD_4$ transient. To produce an HD or D_2 transient, however, the surface was titrated with H_2. As will be demonstrated below, reduction of surface species proceeds more slowly with H_2 than D_2, resulting in a distortion in the time scale of the HD/D_s transient relative to the $^{13}CD_4/C_s$ or $^{13}CD_4/CO_s$ transients. This distortion is so severe that the maximum in the D_β portion of the HD transient aligns coincidently with the maximum in the $^{13}CD_4/CO_s$ transient. To compare the reduction transients for different surface species properly, transients resulting only from the reduction of the surface with D_2, or only from the reduction with H_2, must be used. The appropriate D_2 reduction transients are shown in Fig. 10, and the H_2 reduction transients in Fig. 11.

In both Figs. 10 and 11, the β-peak in the HD transient occurs 5 to 10 s before the peak in the $^{13}CD_4/C_s$ or $^{13}CH_4/C_s$ transient. This suggests the rate of D (or H) exchange with a carbon-containing species such as CH_{x_s} (or CD_{x_s}) is more rapid than the rate at which carbon is removed from the surface as methane. The relationship of these processes can be represented by the following scheme:

$$\begin{tikzcd}
CD_{x_s} \arrow[r, "H_s", "\text{fast}"'] \arrow[d, "H_s"', "\text{slow}"] & CH_{x_s} + HD \arrow[d, "H_s"', "\text{slow}"] \\
CD_xH_{4-x} & CH_4
\end{tikzcd}$$

This scheme also provides an explanation for the absence of any methane containing both H and D atoms.

It is important to note that when comparing the rates of accumulation of surface species during varying lengths of reaction, the reactions must be conducted with either H_2 or with D_2 as was done for Fig. 4. Otherwise, the accumulation rates of the surface

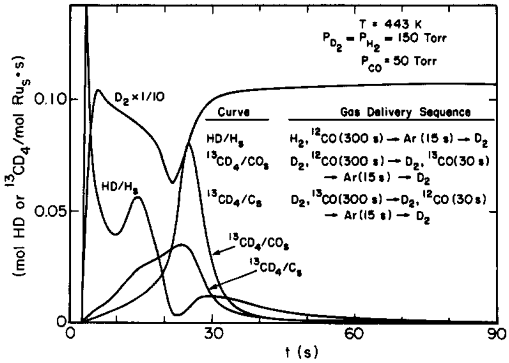

FIG. 10. Transient responses observed during titration of catalyst surface with D_2 following a period of time under reaction conditions.

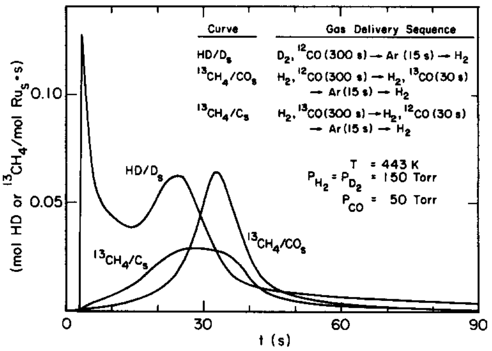

FIG. 11. Transient responses observed during titration of catalyst surface with H_2 following a period of time under reaction conditions.

TABLE 2[a]

Feed stream	θ_D[b]	θ_C[c]	θ_{CO}	D_β/C_β
H_2, CO	1.8	0.8	0.9	1.1
D_2, CO	2.4	0.7	0.8	2.4

[a] $T = 443$ K, $P_{H_2} = P_{D_2} = 150$ Torr; $P_{CO} = 50$ Torr; length of reaction = 300 s.

[b] Total accumulation of deuterium or hydrogen.

[c] Total of all carbon forms.

species will be affected by the H_2/D_2 isotope effect during the steady-state reaction.

The influence of using H_2, rather than D_2, on the inventory of hydrogen (deuterium) following 300 s of reaction is given in Table 2. The ratio of coverages for D_α and H_α is 0.9, in good agreement with estimates based on transition-state theory presented by Kellner and Bell (*14*). By contrast, the ratio of surface concentrations for D_β and H_β is 2.3. Since the inventory of C_β is unaffected by the choice of hydrogen isotope, H_β/C_β is significantly smaller than D_β/C_β. The direction of the isotope effect on the hydrogen to carbon ratio on the C_β deposit suggests that the hydrogenation of C_β is a reversible reaction which is close to being at equilibrium. As discussed by Kellner and Bell (*14*), the equilibrium constant for the processes such as

$$C_s + xD_s \rightleftarrows (CD_x)_s$$

is greater for deuterium than for hydrogen.

The variation in the gas phase concentration of the reducing gas, D_2, is shown in Fig. 10 as a function of reduction time. A substantial consumption of D_2 occurs during the reduction, as noted by the minimum which occurs in its concentration. This consumption is so severe that the rate of H_2/D_2 exchange slows down sufficiently to generate a dip in the HD transient at about 22 s. The total consumption of H_2 (or D_2) during reduction can be determined by integrating the difference between the observed H_2 (or D_2) concentration and that in the reactor inlet. The H_2 or D_2 consumption measured this way is 7.2 monolayer equivalent. This value agrees reasonably well with the value of 6.7 monolayer equivalents determined by calculating the H_2 or D_2 consumed by the following reactions:

$$D_s + 0.5\, H_2 \rightarrow HD$$
$$CO_s + 3H_2 \rightarrow CH_4 + H_2O$$
$$C_s + 2H_2 \rightarrow CH_4$$
$$2S + 1.65H_2 \rightarrow 2H^*_{1.65_s}$$

(* includes physisorbed H_2).

Reversibility of CO Dissociation

Earlier, an analysis was presented which determined the surface concentration of C_α by modeling the decline in $^{13}CD_4$ rate following a switch from D_2–^{13}CO to D_2–^{12}CO. This required that the only reaction pathway for the removal of carbon from the C_α pool was its conversion to hydrocarbons. The reassociation of the C_α with surface oxygen was not considered. The following set of experiments were conducted to compare the relative rates of C_α conversion to hydrocarbons with the reassociation of C_α with surface oxygen to form CO.

The catalyst was initially flushed with argon for 10 min to desorb adsorbed deuterium. A 50:50 mixture of $C^{18}O$: ^{13}CO was then passed over the catalyst for 60 s to saturate the surface. The isotopic composition of the $C^{18}O$ was 1% $^{12}C^{16}O$, 99% $^{12}C^{18}O$, and the ^{13}CO was 17% $^{13}C^{18}O$, 83% $^{13}C^{16}O$. The catalyst was then flushed in argon for up to 240 s during which time the CO isotopes could either desorb, be converted to CO_2, or dissociate and reassociate. Following the scrambling period, the catalyst was flushed with $^{12}C^{18}O$, to displace the $^{13}C^{16}O$, $^{13}C^{18}O$, and excess $^{12}C^{16}O$. The production of CO_2 could be determined by reducing the catalyst with D_2 following the introduction of $^{12}C^{18}O$. The amount of $^{13}CD_4$ formed was taken to correspond to the amount of CO_2 formed during the initial

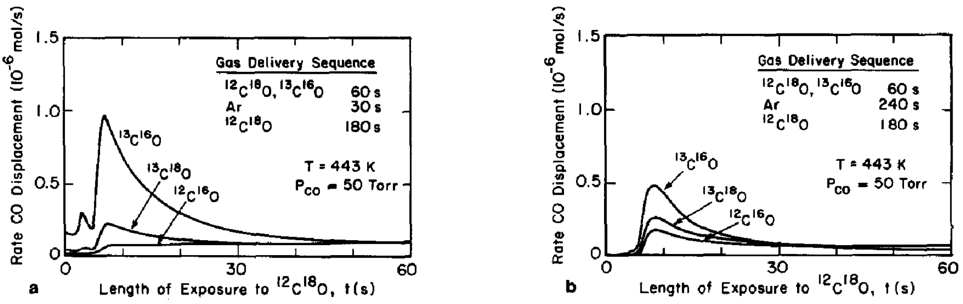

FIG. 12. Displacement of CO isotopes from catalyst surface following varying lengths of flushing with argon. Sequencing as follows: Ar → $^{12}C^{18}O$, $^{13}C^{16}O$ (60 s) → Ar (varies) → $^{12}C^{18}O$ (60 s). Length of argon flush: (a) 30 s (b) 240 s.

phase of the experiment, under the assumption that carbon is released via the Boudouard reaction. The amount of carbon produced via the dissociation of adsorbed $^{12}C^{18}O$ could not be measured directly, and so was estimated from the measured population of the surface by the other species.

The CO isotope displacement transients following 30 and 240 s of argon flushing are shown in Figs. 12a and b. The tailing of these transients is due to the adsorption and desorption of CO in the mass spectrometer. Following 30 s of argon flushing, no significant isotope scrambling was observed. The amount of $^{13}C^{16}O$, $^{13}C^{18}O$, and $^{12}C^{16}O$ desorbed, plus the $^{12}C^{18}O$ not observable, represent a dispersion of 0.39%, in good agreement with hydrogen chemisorption and CO titration experiments. Following 240 s of argon flush, the size of the $^{13}C^{16}O$ transient decreased while the $^{13}C^{18}O$ and $^{12}C^{16}O$ transients increased. The total amount of CO_s desorbed decreased by 30% due to desorption and conversion to CO_2. By carbon and oxygen balances it is possible to estimate the initial and final CO isotope surface concentrations shown in Table 3. For a decrease in the amount of $^{12}C^{18}O$ and $^{13}C^{16}O$, there is a corresponding increase in the amount of $^{12}C^{16}O$ and $^{13}C^{18}O$.

Based on the results given in Table 3, the rates of CO desorption, CO_2 production, and CO isotope scrambling are estimated as follows:

$$\text{Rate of CO desorption} = 1 \times 10^{-3}\ \text{s}^{-1}$$
$$\text{Rate of } CO_2 \text{ production} = 1 \times 10^{-4}\ \text{s}^{-1}$$
$$\text{Rate of } ^{12}C^{18}O\text{–}^{13}C^{16}O \text{ scrambling} = 1\text{–}2 \times 10^{-4}\ \text{s}^{-1}$$

It is apparent that the rates of CO_2 production and isotopic scrambling are an order of magnitude slower than the rate of CO desorption. The first two processes are also on an order of magnitude slower than the rate of CO consumption during Fischer–Tropsch synthesis, 2×10^{-3} s^{-1}. Since the surface concentration of oxygen during Fischer–Tropsch synthesis will be even lower than in the isotopic scrambling experiments, due to the very rapid reaction of surface oxygen to form water, the rate of isotopic scrambling under synthesis conditions is expected to be very small.

DISCUSSION

The present study demonstrates that by suitable use of isotopically labeled reac-

TABLE 3[a]

Argon flush (s)	$^{12}C^{16}O$	Surface composition (%)		
		$^{13}C^{16}O$	$^{12}C^{18}O$	$^{13}C^{18}O$
30	1	42	49	8
240	7	36	43	14

[a] $T = 443$ K; $P_{CO} = 50$ Torr.

tants, it is possible to determine quantitatively the amounts of carbon monoxide, hydrogen, and carbon present on the surface of unsupported Ru during CO hydrogenation. It is also established that such studies can reveal the presence of multiple forms of a given species.

While the mode of CO adsorption on Ru powder was not identified in the current work, its structure can be inferred from previous investigations. Infrared spectra of CO adsorbed on low dispersions of Ru supported on silica and alumina (*7, 10, 17*) and on Ru single crystal surfaces (*18*) clearly indicate that CO adsorbs predominantly in a linear fashion. The same is, therefore, assumed for the Ru powder. This conclusion is further supported by the measurements of H_2 and CO chemisorption, discussed earlier, which shows two moles of CO are adsorbed per mole of H_2.

The rate of dissociation of CO to adsorbed carbon and oxygen and their reassociation to CO was studied using isotope scrambling methods. These results demonstrated that the rate of reassociation of surface carbon and oxygen is substantially less than the rate of hydrocarbon synthesis. Therefore adsorbed carbon species are removed from the surface only in the form of hydrocarbons. The low rate of CO equilibrium on Ru powder is in agreement with results by Bossi *et al.* (*19*) for Ru/SiO_2. While Bossi *et al.* reported that the rate of isotopic scrambling over Ru/Al_2O_3 is rapid, this result must be questioned since scrambling could have occurred through the formation of formate species on the surface of the alumina support.

The most striking observation of the present study is that the catalyst maintains a large inventory of deuterium under reaction conditions. The portion of the total inventory attributable to atomically adsorbed D_2 on the Ru surface is equivalent to about 0.8–0.9 of a Ru monolayer. The coexistence of such a high concentration of adsorbed D_2 with nearly a monolayer of adsorbed CO is remarkable but not unprecedented. McKee (*13*) has reported that at temperatures between 318 and 427 K, Ru powder will coadsorb nearly a monolayer of CO together with two monolayers, or more, of atomic hydrogen. While McKee assumed that all of the H_2 taken up was due to adsorption on the metal, this may not be completely correct. Above 373 K, noticeable amounts of CH_4 were found to build up in the adsorption apparatus, indicating that hydrogenation of CO could not be avoided. The present investigation has shown that under such circumstances carbon will accumulate rapidly on the catalyst and that this carbon can contain some hydrogen. Since McKee's measurements of H_2 and CO uptake were made 5 min after exposure of the catalyst to the H_2–CO mixture, it is very likely that some accumulation of carbon did occur, contributing to enhanced H_2 adsorption. The coexistence of 0.6 of a Ru monolayer of adsorbed H atoms, together with a monolayer of adsorbed CO, has been reported by Kobori *et al.* (*9*) at the outset of CO hydrogenation at 423 K over Ru/SiO_2.

There are some indications in the literature that adsorbed CO may strengthen the chemisorption of H_2 on Ru. Goodman *et al.* (*20*) noted a 2–3 kcal/mole increase in the H_2 binding energy when CO was added to a Ru(110) surface saturated with H_2. Evidence for a weak attractive H–CO interaction have also been reported by Kraemer and Menzel (*21*) and by Vickermann and Christmann (*22*). Peebles *et al.* (*23*) and White (*24*) have suggested that the strength of such interactions may very likely depend on the structure of the exposed metal surface, being stronger on the more open than the close-packed surface.

The results of this study agree with the conclusion of our earlier study on Ru/SiO_2 (*10*) that C_α is the primary form of carbon responsible for the synthesis of methane and higher molecular weight hydrocarbons. Both studies have shown that C_α comprises a small fraction of the total inventory of carbon on the catalyst, and that the coverage by C_α is independent of time under reaction conditions. A further point of agreement is that the steady-state rate of methane synthesis is proportional to the coverage by C_α.

The principal portion of the carbon accumulated on the surface of Ru powder can be removed by reduction with D_2 (or H_2) but does not participate directly in the synthesis process. This is the form designated as C_β by Winslow and Bell (*10*) in their studies of CO hydrogenation over Ru/SiO_2. In contrast to C_α, the inventory of C_β increases steadily with time under reaction conditions (see Fig. 6). The near parallel growth in the inventories of deuterium and carbon strongly suggest that C_β is associated with a significant amount of deuterium. As noted earlier, the ratio of D_β/C_β lies between 1.8 and 2.4, increasing with time under reaction conditions. The assignment of C_β to a hydrocarbon species is supported by recent ^{13}C-NMR spectra obtained by Duncan *et al.* (*12*). These spectra exhibit a peak at -15 ppm which is attributed to alkyl species attached to the Ru surface. It is important to note, though, that at temperatures higher than 443 K, or in the presence of H_2 rather than D_2, the hydrogen to carbon ratio of C_β can fall below 2.0, suggesting that not all of the carbon atoms in the C_β deposit are fully hydrogenated.

The structure and composition of C_β, and its reactivity upon reduction, closely resemble the characteristics of adsorbed hydrocarbon species observed by Tamaru and co-workers (*8, 9*) during CO hydrogenation over Ru/SiO_2. Their studies revealed the progressive accumulation of a carbonaceous deposit on the catalyst surface which did not inhibit the chemisorption of CO nor the steady-state synthesis of hydrocarbons. Following 100 min of reaction at 423 K, the deposit corresponded to ~0.4 of a Ru monolayer. The H/C ratio of the deposit was roughly 1.6. Infrared spectra of the deposit showed evidence for CH_2 and CH_3 groups. From the spectra it was estimated that the deposit consists of a relatively small number of hydrocarbon chains containing 4 to 30 carbon atoms, the number of carbon atoms increasing with reaction time. The absence of any effect of hydrocarbon accumulation on the adsorption of CO was ascribed to the small number of sites required for attachment of the hydrocarbon chains. Finally, it was noted that upon reduction of the carbonaceous deposit only CH_4 was formed, suggesting that the hydrocarbon chains undergo rapid C–C bond scission to form individual carbon atoms.

The correspondence between the species observed by Tamaru and co-workers (*8, 9*) and C_β is further strengthened by the results reported by Winslow and Bell (*10*). In that study, C_β was observed to accumulate progressively on a Ru/SiO_2 catalyst during steady-state CO hydrogenation. While the hydrogen content of C_β was not determined, recent ^{13}C-NMR studies by Duncan *et al.* (*12*) have demonstrated that at least part of the C_β species on Ru/SiO_2 consists of alkyl chains. Winslow and Bell (*10*) also noted that in agreement with the work of Tamaru and co-workers the kinetics of hydrocarbon species (i.e., C_β) accumulation are positive order in the partial pressures of both CO and H_2.

The hydrogenation of C_β results primarily in the formation of methane indicating that the hydrocarbon chains comprising C_β undergo chain scission prior to the reduction of the carbon. Infrared studies carried out by Tamaru co-workers (*8, 9*) with Ru/SiO_2 indicate that the bond scissioning process will occur even in the absence of hydrogen, since the intensity of the C–H stretching bonds attenuate without the release of hydrocarbon products. Winslow and Bell (*10*) have also reported recently that C_β on Ru/SiO_2 will gradually convert to C_α when maintained at reaction temperature in a flow of helium.

The progressive displacement of the $^{13}CD_4/C_s$ transients to longer times with increasing reaction time, seen in Fig. 5b, can now be explained as follows. The longer the reaction time, the longer will be the hydrocarbon chains comprising C_β. Since the removal of these chains during reduction necessitates the cleavage of individual C–C bonds in the chains, the removal of C_β will be delayed the longer the chain length. The same explanation would account for the progressive shift of the D_β portion of the HD/D_s transients, shown in Fig. 5c. In this case, it is presumed that H_2–D_2 exchange will not occur until the CD_x species in a chain has become attached to the Ru surface.

The extent to which the accumulation of C_β is responsible for the decrease in synthesis activity, seen in Fig. 1, is difficult to determine. Clearly, there is a correlation between the accumulation of C_β and a decline in the methanation rate; however, a decrease in the coverage of the metal surface by atomic hydrogen does not occur. Whether the suppression of CO chemisorption is responsible for the decline in synthesis activity, or whether the accumulation of C_β inhibits one or more of the elementary steps involved in the synthesis process cannot be established by the present results.

CONCLUSION

Two forms of carbon are observed to coexist on the surface of unsupported Ru powder during CO hydrogenation. The more reactive form, C_α, rapidly achieves a steady state concentration, while the concentration of the less reactive form, C_β, grows progressively with time. The rate of methane synthesis is directly proportional to the surface coverage by C_α. The C_β deposit contains deuterium ($D/C \sim 1.8$ and 2.4) and is believed to exist, at least in part, in the form of hydrocarbon chains. The exchange of hydogen for deuterium bonded to C_β occur more rapidly than the removal of C_β as methane during hydrogenation of the catalyst. A monolayer of CO and a monolayer of D atoms are also present on the catalyst surface under reaction conditions.

ACKNOWLEDGMENT

This work was supported by the Division of Chemical Sciences, Office of Basic Energy Sciences, U.S. Department of Energy under DE-AC03-76SF0098.

The submitted manuscript has been authored by a contractor of the U.S. Government under Contract DE-AC03-76SF00098. The U.S. Government's right to retain a nonexclusive royalty-free license in and to the copyright covering this paper, for governmental purposes, is acknowledged.

REFERENCES

1. Ponec, V., and van Barneveld, W. A., *Ind. Eng. Chem. Prod. Res. Dev.* **18,** 268 (1979).
2. Bell, A. T., *Catal. Rev. Sci. Eng.* **23,** 203 (1981).
3. Biloen, P., and Sachtler, W. M. H., *Adv. Catal.* **30,** 165 (1981).
4. Rofer-de Porter, C. K., *Chem. Rev.* **81,** 447 (1981).
5. Biloen, P., Helle, J. N., and Sachtler, W. M. H., *J. Catal.* **58,** 95 (1979).
6. Biloen, P., Helle, J. B., van de Berg, F. G. A., and Sachtler, W. M. H., *J. Catal.* **81,** 450 (1983).
7. Cant, N. W., and Bell, A. T., *J. Catal.* **73,** 257 (1982).
8. Yamasaki, H., Kobori, Y., Naito, S., Onishi, T., and Tamaru, K., *J. Chem. Soc. Trans. I* **77,** 2913 (1981).
9. Kobori, Y., Yamasaki, H., Naito, S., Onishi, T., and Tamaru, K., *J. Chem. Soc. Trans. I* **78,** 1473 (1982).
10. Winslow, P., and Bell, A. T., *J. Catal.* **86,** 158 (1984).
11. Duncan, T. M., Winslow, P., and Bell, A. T., *Chem. Phys. Lett.* **102,** 163 (1983).
12. Duncan, T. M., Winslow, P., and Bell, A. T., in press.
13. McKee, D. W., *J. Catal.* **8,** 249 (1967).
14. Kellner, C. S., and Bell, A. T., *J. Catal.* **67,** 175 (1981).
15. Kobori, Y., Naito, S., Onishi, T., and Tamaru, K., *J.C.S. Chem. Commum.* 92 (1981).
16. Dalla Betta, R. A., and Shelef, M., *J. Catal.* **49,** 383 (1977).
17. Kellner, C. S., and Bell, A. T., *J. Catal.* **71,** 296 (1981).
18. Pfnur, H., Menzel, K., Hoffman, F. M., Ortega, A., and Bradshaw, A. M., *Surface Sci.* **93,** 431 (1980).
19. Bossi, A., Garbassi, F., Petrini, G., and Zanderighi, L., *Proc. 7th Int. Cong. Cat.*, 1468 (1980).
20. Goodman, D. W., Madey, T. E., Ono, M., and Yates, J. T., Jr., *J. Catal.* **50,** 279 (1977).
21. Kraemer, K., and Menzel, D., *Ber. Bunsenges. Physik. Chem.* **79,** 649 (1978).
22. Vickermann, H. C., and Christmann, K., *Surface Sci.* **120,** 1 (1982).
23. Peebles, D. E., Schriefels, J. A., and White, J. M., *Surface Sci.* **116,** 117 (1982).
24. White, J. M., *J. Phys. Chem.* **87,** 915 (1983).